A&A 487, 453–460 (2008)
DOI: 10.1051/0004-6361:200809600

Astronomy & Astrophysics

The bright galaxy population of five medium redshift clusters⋆

I. Color–magnitude relation, blue fractions, and visual morphology

B. Ascaso[1], M. Moles[1], J. A. L. Aguerri[2], R. Sánchez-Janssen[2], and J. Varela[1]

[1] Instituto de Astrofísica de Andalucía-CSIC, Camino Bajo de Huetor 50, CP 18008 Granada, Spain
e-mail: [ascaso;moles;jesusvl]@iaa.es
[2] Instituto de Astrofísica de Canarias, C/ via Láctea S/N CP La Laguna, Spain
e-mail: [jalfonso;ruben]@iac.es

Received 18 February 2008 / Accepted 28 May 2008

ABSTRACT

Aims. Using data from five clusters of galaxies within the redshift range $0.15 \leq z \leq 0.25$, imaged with the Nordic Optical Telescope (NOT) in the central $\approx$1 Mpc^2 in very good seeing conditions, we have performed an exhaustive inspection of their bright galaxy population. That range of redshift, where only a small amount of data with the required resolution and quality is available, is particularly important for the understanding of the formation and evolution of clusters of galaxies.
Methods. We have inspected the color−magnitude relation (CMR) for those clusters and measured the blue fraction of galaxies in their cores to check for evidence of evolution as found in other works. Visual classification of the galaxy morphology has been performed and the morphology-radius relation examined.
Results. We have not found signs of evolution either in the slope of the CMR or in the blue fraction of galaxies. A diversity of situations regarding those parameters and in the morphological mixing has been noticed, with two out of five clusters containing a dominant late-type core population. The cluster A1878 stands out as some of its properties differ from those of the other clusters in the sample.
Conclusions. No clear signs of evolution appear in our analysis. The data support the view that the morphology and the stellar content of the galaxies in our clusters already have been settled at $z \sim 0.2$. Only the fraction of interacting galaxies in the clusters appear to be larger than in clusters like Coma, although the number of clusters in the sample is too small to give a definitive conclusion.

Key words. cosmology: observations – galaxies: clusters: general – galaxies: fundamental parameters

1. Introduction

Clusters of galaxies are the largest structures in the Universe that are gravitationally bounded. They are crowded with hundreds to thousands of galaxies. Numerous studies have been devoted to the formation of clusters of galaxies. However, two main scenarios still remain. On the one hand, we have the monolithic scenario in which the clusters were formed first (Bower et al. 1998) and on the other, we have the hierarchical scenario (De Lucia & Blaizot 2007b; Kauffmann et al. 1994), in which the galaxies were formed at the outset. The monolithic scenario implies that the galaxies do not undergo substantial transformations after the cluster collapse (Merritt 1984) while the hierarchical scenario would imply that the environmental effects and interactions are transforming the galaxy population due to mechanisms that were operational until recent epochs, such as harassment (Moore et al. 1996), gas-stripping (Gunn & Gott 1972; Quilis et al. 2000), starvation (Bekki et al. 2002), or merging (Gerhard & Fall 1983; Aguerri et al. 2001; Eliche-Moral et al. 2006).

Likewise, the evolution of the galaxy population in clusters of galaxies has been broadly studied in many works. Some of the results found to date are the lower fraction of lenticular galaxies and the larger fraction of late type galaxies found in the cores of higher redshift clusters (Fasano et al. 2000; Dressler et al. 1997). The possible evolution of the slope of the color-magnitude relation (CMR) has also been widely explored (López-Cruz et al. 2004; Driver et al. 2006; Mei et al. 2006; De Lucia et al. 2007a). The agreed result is that the CMR does not change with redshift at least up to redshift $z \sim 1$. This feature is interesting in itself because it gives information about the metallicity and age of the galaxy population (Kodama 1999).

Another attribute that is considered in the context of the evolution of clusters of galaxies is the blue fraction of the galaxy population in clusters. In the early work by Butcher & Oemler (1984), an increase of this blue fraction with redshift was found for clusters up to redshift $\approx$0.5. That fact indicates that the galaxy population would be evolving. However, as shown by Aguerri et al. (2007), that variation would happen only for a limited redshift range. They studied a large sample of SDSS clusters up to redshift $z \leq 0.1$ and did not see any significant change of the blue fraction with the redshift. Therefore, exploring the next redshift range, $0.1 \lesssim z \lesssim 0.3$, would be needed to clarify the situation, since several works have explored and noticed the Butcher-Oemler effect in samples of clusters at lower (De Propris et al. 2004) and higher (De Lucia et al. 2007a) redshift.

Few works have been dedicated to study the morphology of the galaxy population at $z \approx 0.2$. Morphological studies generally have been confined to rather local samples, in part due to the need to establish a visual classification (Dressler 1980; Fasano et al. 2000) and more generally, to the difficulties in obtaining deep and high-resolution images for relatively large fields. Some of these studies have tried to establish an automatic

⋆ Appendix A is only available in electronic form at http://www.aanda.org

morphological classification by inspecting the galaxy surface brightness and main structural parameters. Nevertheless, those samples often have been preselected to be only late type (de Jong 1996; Graham & de Blok 2001) or early type (Graham & Guzmán 2003). As a consequence, the present number of clusters that have been studied in that redshift range is small (Fasano et al. 2000; Trujillo et al. 2001; Fasano et al. 2002).

That range of redshift, however, should be inspected to link the results found for local clusters and for more distant objects that can be explored with the Hubble Space Telescope (HST). There is much evidence indicating that some properties of the clusters and their galaxies could change between the local and ~0.4 redshift ranges.

In the present work we have studied five clusters of galaxies in a range of redshift from 0.15 to 0.25, observed with NOT at La Palma in two bands: Gunn-r and Bessel B, under very good seeing conditions. The clusters presented in this paper were considered by Fasano et al. (2000, 2002) for their study of morphological mixing. They found that, for galaxies with $M_V \leq -20$, the fraction of S0 galaxies was lower for higher z clusters. Here we have analyzed the main characteristics of the bright galaxy population in the central part of those five clusters. We are interested in the possible evolution with z of properties of the galactic populations such as the CMR, the fraction of blue galaxies or the radial distribution of the different (visually determined) morphological types. We have used as templates at lower redshift the results obtained for galaxy clusters at $z \leq 0.12$ by De Propris et al. (2004) for comparison. The analysis of the surface brightness distribution and quantitative morphology of the galaxies will be presented in a forthcoming paper, (Ascaso et al. 2008, in preparation).

The structure of this paper is as follows. In Sect. 2 we present the data, including a brief description of the cluster environment and explain the observations and the reduction process. In Sect. 3, we describe how the galaxies were detected and extracted. Section 4 is devoted to the study of the color-magnitude diagrams and the Butcher-Oemler effect. Section 5 is dedicated to the study of the morphology of the galaxies from a qualitative point of view. We have considered several aspects such as the morphology-radius relation, the concentration parameter and the frequency of interaction systems in our sample. We present the discussion and conclusions in Sect. 6. Throughout the paper we have adopted the standard ΛCDM cosmology with $H_0 = 71$ km s^{-1} Mpc^{-1}, $\Omega_m = 0.27$ and $\Omega_\Lambda = 0.73$.

2. Observations, data reduction and description of the selected clusters

Two of us (M.M. and J.A.L.A.) imaged five galaxy clusters with the 2.5 m Nordic Optical Telescope (NOT) located at the Roque de Los Muchachos Observatory (La Palma). The observations were taken with the Stand Camera, with a field of view of $3' \times 3'$, a plate scale of 0.176″/pix, a gain of 1.69 e$^-$/ADU and a readout noise of 6.36 e$^-$. All images were taken under photometric sky conditions and very good seeing (between 0.5″ and 0.8″).

The clusters were observed through two broad-band filters: Gunn-r' (r) and Bessel B (B). At least two exposures for each field in each filter were usually taken, allowing us to clean the combined images of cosmic-rays and spurious events. The data reduction and calibration was performed as presented in Fasano et al. (2002). Here we summarize the basic steps of the data reduction process; for more information we refer the reader to Fasano et al. (2002).

The bulk of the data reduction of the images was achieved using standard IRAF tasks. The electronic bias level was removed from the CCD by fitting a Chebyshev function to the overscan region and subtracting it from each column. By averaging ten bias frames, a master bias per night was created and subtracted from the images in order to remove any remaining bias structure. Dark images were also observed in order to remove the dark signal from the CCD. This correction turned out to be negligible, and was not considered. Twilight flats were also observed at the beginning and at the end of each observing night. They were combined and used to remove the pixel-to-pixel structure of the images.

The photometric calibration of the images was obtained by observing several standard stars from the Landolt (1992), Jorgensen (1994), and Montgomery et al. (1993) catalogues. They were observed each night at different zenith distances in order to measure the atmospheric extinction. The calibration constant was taken from Fasano et al. (2002).

2.1. Cluster environment

Given the scarce information on the clusters presented here, we comment briefly on the redshift data and the environmental situation of each of them.

A1643. The redshift of this cluster is attributed by Humason et al. (1956), who obtained a spectrum of the brightest galaxy in the area, finding $z = 0.198$. Our images were centered at that position α(J2000) = 12h55m54.4s, δ(J2000) = +44d04m46s. More recently, Gal et al. (2003) detected an overdense region centered at α(J2000) = 12h55m42.4s, δ(J2000) = +44d05m22s, identified as cluster NSC J125542+440522. They have determined a photometric redshift of 0.2515. Both clusters appear in our frames where we can identify A1643 as the one dominated by the galaxy observed by Humason et al. (1956) and, therefore, at $z = 0.198$. This is the value we adopt in this paper. We will exclude the frames that could be contaminated by the presence of NSC J125542+440522 in all the analysis regarding the galactic content of A1643.

A1878. This clusters appears with $z = 0.254$ in the NED[1]. A closer inspection shows that there is another value given to a galaxy in the field, namely $z = 0.222$. Both redshift values come from Sandage et al. (1976), who observed the brightest galaxy in the field, placed at α(J2000) = 14h12m52.13s, δ(J2000) = +29d14m29s, and another, fainter galaxy at α(J2000) = 14h12m49.13s, δ(J2000) = +29d12m59s. As quoted by the authors, the spectra were of low quality. The low z value corresponds to the brightest object that appears at the center of a strong concentration of galaxies that correspond to the cluster catalogued as A1878. More recently, Gal et al. (2003) identified a cluster labeled as NSC J141257+291256, with a photometric redshift $z = 0.22$. Its position and redshift value coincide with that of the bright galaxy observed by Sandage et al. (1976) that is accepted here as the brightest galaxy of A1878.

A1952. The redshift attributed to this cluster, $z = 0.248$, also comes from the work by Sandage et al. (1976) who observed the brightest cluster galaxy. The possible confusion regarding this cluster comes from the fact that the position given by Abell et al. (1989), α(J2000) = 14h41m04.2s, δ(J2000) = +28d38m12s, does not coincide with that of its Brightest Cluster Galaxy (BCG) as given by Sandage et al. (1976), α(J2000) = 14h41m03.6s, δ(J2000) = +28d36m59.68s. To add to the confusion, Gal et al. (2003) detected a cluster designed

[1] NASA/IPAC Extragalactic Database.

Table 1. The sample of clusters.

Name	α(2000)			δ(2000)			z	# frames	Area (Mpc^2)	seeing ($''$)
A 2658	23	44	49	–12	17	39	0.185	1	0.3055	0.70
A 1643	12	55	54	+44	05	12	0.198	2	0.6810	0.55
A 1878	14	12	52	+29	14	28	0.220	2	0.7894	0.70
A 2111	15	39	40	+34	25	27	0.229	2	0.8030	0.70
A 1952	14	41	03	+28	37	00	0.248	2	0.7989	0.55–0.80

by NSC J144103+283622, at almost exactly the position of A1952's BCG, but the redshift they determined photometrically amounts to 0.2084. Taking all the information at hand, we consider that the cluster identified by Gal et al. (2003) is A1952, but the redshift we adopt here is that measured by Sandage et al. (1976), $z = 0.248$. The analysis we present here of the Color-Magnitude Relation support this conclusion.

A2111. This cluster has the largest amount of information available in the literature of all the clusters in our sample. The redshift was established from spectroscopic observations by Lavery & Henry (1986). The center given by NED comes from the ACO catalogue given by Abell et al. (1989), namely, α(J2000) = 15h39m38.3s, δ(J2000) = +34d24m21s. However, the subsequent analysis of the X-ray data by Wang et al. (1997); Henriksen et al. (1999); Miller et al. (2006), led them to conclude that the cluster center position is at α(J2000) = 15h39m40.9s , δ(J2000) = +34d25m04s, only 5.04 kpc away from the Brightest Cluster Galaxy. Miller et al. (2006) also provide a large number of spectra. Interestingly, the X-ray works showed that this cluster is undergoing a merger and presents a rather large blue fraction.

A2658. The redshift is taken from Fetisova (1982). The center, as given by Abell et al. (1989) is at α(J2000) = 23h44m58.8s, δ(J2000) = −12d18m20s. However, our BCG is located at α(J2000) = 23h44m49.83s, δ(J2000) = −12d17m38.93. After a visual inspection of the cluster image in the Digital Sky Survey, we conclude that the center of the cluster is given by the BCG, where a high concentration of galaxies is visually detected.

The adopted central position and redshift value for the five clusters discussed here are collected in Table 1. We also show in the table the details of the observations. Columns 1−4 give the cluster name, center coordinates (right ascension and declination in Equatorial coordinates, J2000) and redshift, respectively. The number of pointings observed for each cluster are indicated in Col. 5. These pointings cover the different cluster areas shown in Col. 6. The last column gives the seeing of the observed images. For the center position we adopted that of their respective BCGs except for A2111, for which the X-ray data has been used.

3. Galaxy detection and extraction

We used SExtractor (Bertin & Arnouts 1996) to detect the individual objects in our images, and to extract their photometric parameters. The extraction of the galaxies was performed on the deeper Gunn-r images. The photometry of the galaxies in the B-band was obtained using the ASSOC mode of SExtractor. We fixed several SExtractor parameters based on the properties of the images, such as: background level, stellar FWHM, zero-point, exposure time, or radius for aperture photometry. The values of the other SExtractor parameters such as the minimum area of pixels above threshold (DETECT_MINAREA), the number of deblending sub-thresholds (DEBLEND_NTHRESH) or the minimum contrast parameter for deblending (DEBLEND_MINCONT), were established after checking the results of the deblending images.

Table 2. Photometric errors.

Name	Err Aper	Err Best	Err Col
A 2658	0.007	0.008	0.028
A 1643	0.005	0.006	0.033
A 1878	0.007	0.008	0.052
A 2111	0.007	0.009	0.045
A 1952	0.006	0.007	0.040

In this way, we obtained a first catalogue of 488 objects, including stars and galaxies. The stars were identified using the stellar index given by SExtractor. We considered an object as a galaxy when its stellar index was smaller than 0.2 and as star if the stellar index was larger than 0.8. The objects with intermediate values of the stellarity index were considered as doubtful objects. Only a small fraction of objects were classified as stars (27) or doubtful (5), so the final catalogue includes 456 galaxies.

SExtractor provides different magnitudes for each detected galaxy. We have considered two of them. The first one corresponds to a fixed-aperture of radius five kpc, useful to compare colors in the same physical region (Varela 2004). The other one is the magnitude called by SExtractor "MAG_BEST" that is determined in an automatic aperture that depends on the neighbours around the galaxy. If those neighbours are bright enough to affect the magnitude corresponding to an aperture enclosing the whole object by more than 10%, then that magnitude is taken as the corrected isophotal magnitude, which corresponds to the isophotal magnitude together with a correction. This magnitude provides the best measures of the total light of the objects (Nelson et al. 2002; Stott et al. 2008).

The B- and r- SExtractor magnitudes were k-corrected in the following way. For the B-band filter we adopted the relation $k_B = 4.4225z + 0.0294$, obtained as an interpolation of the data given by Pence (1976) in the range $0.08 \leq z \leq 0.24$. The magnitudes of the Gunn-r filter were k-corrected using the approximation $k_r = 2.5\log(1+z)$ (Jorgensen et al. 1992)

In Table 2 we show the mean r-band magnitude error provided by SExtractor for all the galaxies in each cluster. The last column shows the errors in colour, obtained as the quadratic sum of the errors of the fixed-aperture magnitude in the two filters B and r. For the calibration errors in the Gunn-r band, see Fasano et al. (2002).

4. Properties of the cluster galaxies

4.1. The color–magnitude relation

In the early fifties, Baum (1959) and Rood (1969) realized that the color index of the bright, early type galaxies correlates with their luminosity. Later on, Visvanathan & Sandage (1977) and Visvanathan & Griersmith (1977) concluded on the universality of the so called CMR found for early type galaxies. Since then

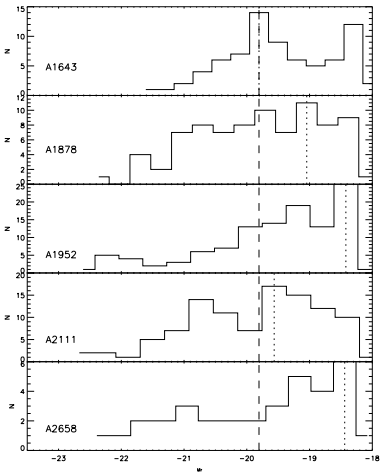

Fig. 1. Absolute magnitude histogram of the galaxies in the five clusters. The dotted line shows the completeness magnitude limit for each cluster; the dashed line shows the common magnitude limit we have adopted for the five clusters.

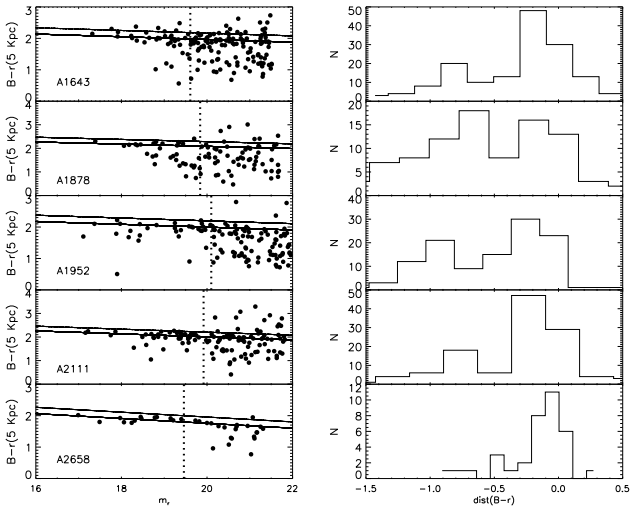

Fig. 2. *Left panels*: the color−magnitude diagrams for the five clusters. The solid line is the fit to the red sequence and the dotted line is the upper 0.2 mag limit. The vertical line corresponds to the limit $M_r = -20$ at the cluster redshift. *Right panels*: the histograms of the $B-r$ distance of the galaxies to the corresponding red sequence.

the study of the CMR has been used as a tool to analyze the evolution with z of the early type galaxies (see for example Driver et al. 2006; De Lucia et al. 2007a).

We present here the CMR for the galaxies found in our clusters. We use the color index $B-r$ measured in a five kpc aperture. For the magnitudes we use the BEST magnitudes provided by SExtractor. All the detected galaxies in each cluster up to some limiting magnitude were used to build the relation. In Fig. 1, we have plotted the absolute magnitude distribution of the sample together with the completeness limit for each cluster and for the whole sample. The completeness limit has been defined as the maximum of the distribution. The sample appears to be complete up to $M_r \approx -19.8$. Therefore, to avoid possible problems with the magnitude limit, we have considered a safer limit. Only galaxies brighter than $M_r = -20$ have been used for the analysis of the CMR.

The definitive criterion to find the galaxies that actually belong to a given cluster is indeed the redshift. Unfortunately, the redshift information is in general scant for clusters at redshift ∼0.2 except for some particular cases. We have found in the literature 22 galaxies in the frame of A2111 with redshift data provided by Miller et al. (2006), whereas for the other clusters there are just one or two redshift entries in the NED. On the other hand, the CMR is well defined and it is not necessary to have the redshift information at hand to analyze it. Background galaxies are identified as those objects that are 0.2 mag redder than the value from the fitted CMR. That value seems safe if we take into account the combined uncertainty of the photometric errors and that $3\sigma \approx 0.1-0.18$. After applying this criterion the final number of galaxies retained as members of one of our five clusters is 408. They are collected in the table presented in the appendix. The first column gives the name of the cluster. The second and third columns give the coordinates of the galaxy, the fourth column gives the z information when available. The fifth and sixth columns give the r and B absolute magnitudes of each galaxy, assuming that they are located at the cluster redshift.

The fit of the red sequence of the CMR for each cluster has been determined by carrying out a least absolute deviation regression fit to the observed data (Armstrong & Kung 1978). The fit of the CMR for each cluster was obtained using an iterative procedure. A first fit was obtained using all the galaxies brighter than $M_r = -20$ for a given cluster. Then, the distance of each galaxy in $B-r$ to the fitted CMR was computed. Those galaxies with a distance greater than three times the rms of the fitted relation were rejected, and a new fit to the CMR was performed with the remaining ones. This process was repeated until the fit to the CMR did not change further. The final fit was estimated using a nonparametric bootstrap method (Efron & Tibshirani 1986), with $n \log^2 n$ resamplings, n being the number of galaxies up to the completeness limit, as presented in Babu & Singh (1983). The slope and zero point are the median value of the resampling, and the standard errors we estimated as the rms of the bootstrap samples. We have checked that the early type galaxies that belong to A2111 are contained in the CMR. In Fig. 2, we show the colour−magnitude diagrams for all the galaxies in the frames and the CMRs fitted for all the clusters. We have also plotted in that figure the histogram of the color differences between the observed and the CMR-fitted values. We give in Table 3 the zero point, a_0, the slope, a_1 and the rms of the fitted CMRs for each cluster.

In Fig. 3, we have plotted the slopes of the fitted CMRs in our clusters at medium redshift together with those obtained by López-Cruz et al. (2004) for clusters with $z < 0.15$. As the figure illustrates, there is no clear tendency of the change in slope of the CMR with redshift. The mean value of the slope of the CMR for our sample together with López-Cruz et al. (2004) is -0.051 ± 0.008, and for our sample only is -0.055 ± 0.014. These values are also very similar to the slope value found by Mei et al. (2006) for two clusters at $z \sim 1.26$. Thus, the slope values we find for our clusters at $z \sim 0.2$ are completely consistent with the values found for lower and much higher redshift values. Moreover, the range of values found at any redshift are also similar. Thus, we find no indication of a change of the CMR slope up to $z \sim 0.25$ and even up to $z \sim 1.26$. This result would indicate that the stellar population of the bright, early type galaxies defining the cluster red sequence was settled soon after the galaxy formation.

4.2. The blue galaxy fraction

We have studied the fraction of blue galaxies, f_b, in the bright population, $M_r \leq -20$, of the clusters presented here. The blue

Table 3. CMR parameters and the galaxy blue fractions.

Name	$a0$	$a1$	rms	f_b (420 kpc)	f_b (735 kpc)
A 2658	3.301 ± 0.257	-0.077 ± 0.013	0.037	0.083 ± 0.079	
A 1643	2.825 ± 0.224	-0.043 ± 0.011	0.035	0.090 ± 0.086	0.090 ± 0.086
A 1878	3.022 ± 0.390	-0.046 ± 0.021	0.060	0.363 ± 0.102	0.517 ± 0.092
A 2111	3.285 ± 0.079	-0.063 ± 0.004	0.053	0.031 ± 0.030	0.125 ± 0.052
A 1952	2.893 ± 0.257	-0.044 ± 0.013	0.009	0.250 ± 0.088	0.285 ± 0.085

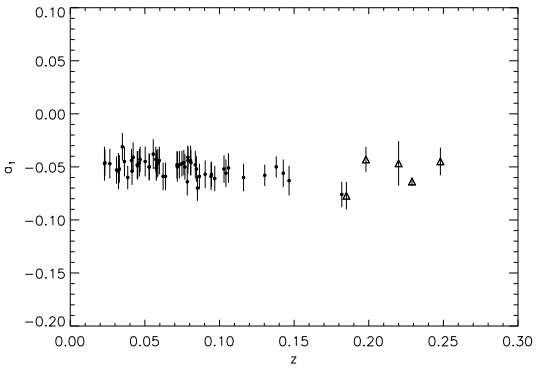

Fig. 3. Slopes of the CMR for the sample of López-Cruz et al. (2004) (black circles) and our sample (empty triangles).

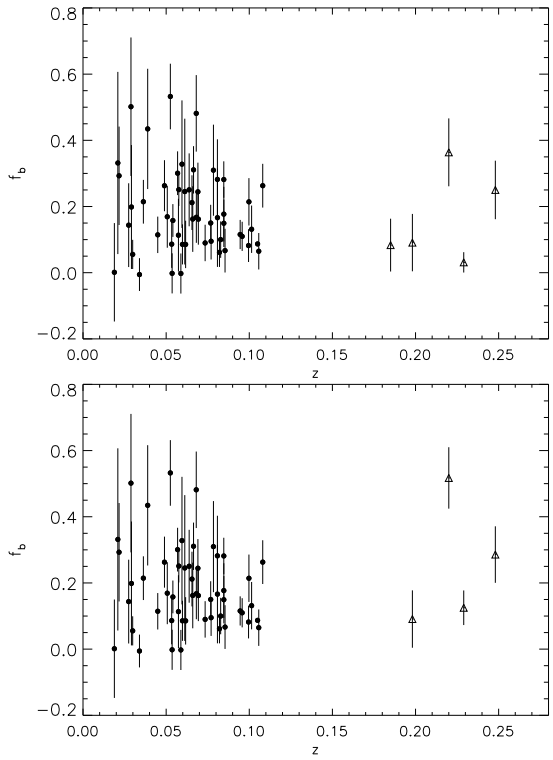

Fig. 4. Blue fraction of galaxies in our sample of clusters (triangles) compared with those obtained by De Propris et al. (2004) (black circles) for an aperture of $r_{200}/2$. *The top (bottom) panel* corresponds to the blue fraction computed within a radius of 420 kpc (735 kpc).

fraction was defined as the ratio of the number of blue galaxies observed out of the total number of galaxies within a fixed aperture. We have considered as blue galaxies those with a $B-r$ color at least 0.26 mag bluer than the red sequence. This color index corresponds to the original definition by Butcher & Oemler (1984), who considered as blue those galaxies whose colors were bluer than $B-V = 0.2$ at $z = 0$. Given the photometric errors and the statistical nature of the k-correction we adopted that common value of the color index for all the five clusters in spite of their differences in redshift. The results are not affected if individual color values were adopted.

The removal of foreground galaxies was done on the base of the measured redshift when available (just very few cases) or using statistical arguments. By integrating the luminosity function of field galaxies up to $M_r = -20$ in the solid angle corresponding to each of our clusters, we obtained 0.38 foreground galaxies per frame at $z = 0.2$. This estimation is in good agreement with previous findings by Fasano et al. (2000). The foreground contamination is therefore statistically negligible. The fraction of blue galaxies has been computed for each cluster using all the surveyed area. In order to be able to compare our results for the different clusters and with other studies, we have considered that our frames are representative of the area corresponding to a circular aperture that, set at the center of the cluster, includes all the area that we have covered. For comparison, we have adopted two apertures, of radius 420 and 735 kpc respectively. For the cluster A2658, only the smaller aperture could be used. Indeed, in the original definition given by Butcher & Oemler (1984), the fraction was calculated for an aperture containing 30% of the cluster population (R_{30}). Since only the central parts of our clusters were sampled we could not determine the value of R_{30} for them. The fixed apertures we have used are a substitute for the canonical value. We notice that they are in the range of the expected R_{30} values as given by Butcher & Oemler (1984). The errors attributed to the measured fractions, listed in the last two columns of Table 3, were computed assuming Poissonian statistics, following De Propris et al. (2004).

In Fig. 4 we show the blue fraction of galaxies in our clusters as a function of redshift within a radius of 420 kpc (top panel) and within a radius of 735 kpc (bottom panel). We have also plotted for comparison the blue fraction of galaxies obtained from a sample of nearby galaxy clusters by De Propris et al. (2004) within an aperture of $r_{200}/2$. As can be seen in the figure, our errors bars are very similar to those given by De Propris et al. (2004). In all cases, we have more than 10 galaxies per cluster to compute the blue fraction. The comparison with the data by De Propris et al. (2004) clearly indicates that there is no relation between the value of the blue galaxy fraction and the cluster redshift.

The range of values found is also similar to that found by De Propris et al. (2004) for lower redshift clusters. In particular, the very high blue fraction we obtain for A1878 is found for some lower z clusters in the quoted reference. The central median values we find for our sample are $\langle f_b \rangle = 0.090 \pm 0.138$ for the 420 kpc and 0.285 ± 0.194 for the 735 kpc aperture, in agreement with the median f_b value, 0.162 ± 0.125 of De Propris et al. (2004), for an aperture of $r_{200}/2$.

We find a nominal increment in the blue fraction as a function of the aperture. This is in agreement with the findings

Table 4. Fraction of morphological types.

Name	420 kpc				735 kpc			
	E	*S*0	*S*	*I*	*E*	*S*0	*S*	*I*
A 2658	0.54	0.31	0.15	0.00				
A 1643	0.22	0.22	0.56	0.00	0.24	0.19	0.57	0.00
A 1878	0.11	0.22	0.41	0.26	0.14	0.24	0.43	0.19
A 2111	0.38	0.28	0.28	0.00	0.35	0.28	0.30	0.08
A 1952	0.52	0.28	0.20	0.00	0.45	0.31	0.24	0.00

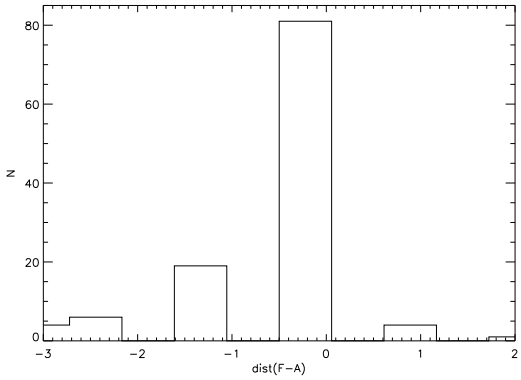

Fig. 5. The visual classification differences between Fasano et al. (2000) and this paper.

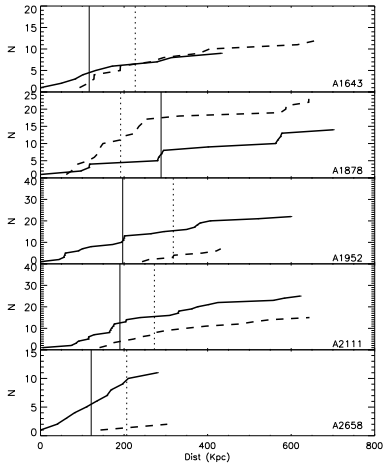

Fig. 6. Cumulative functions of the different morphological types as a function of the projected radius to the center of the cluster. Early types: solid lines; late types: dotted lines. The vertical lines indicate the radius where the distributions reach the 50% level.

by Margoniner & de Carvalho (2000); Goto et al. (2003); De Propris et al. (2004).

Regarding the cluster A2111, Butcher & Oemler (1984) obtained a blue fraction of 0.16 ± 0.03 within a r_{30} that, for this cluster, corresponds to 892 kpc. Miller et al. (2006) obtained, for the same aperture, the values of 0.15 ± 0.03 and 0.23 ± 0.03 using photometric data or only galaxies with spectroscopic data, respectively. We have obtained 0.031 ± 0.030 and 0.125 ± 0.052 for our 420 kpc and 735 kpc aperture, a smaller value, in agreement with the smaller aperture, even if not significantly different when the errors are taken into account.

5. Galaxy morphology

For the analysis presented here, we have classified the galaxies visually. A quantitative analysis will be presented in a forthcoming work (Ascaso et al. 2008).

All the galaxies brighter than $M_r = -20.0$ were classified visually by two of us (B.A. and J.V.) into four different types: Ellipticals (E), Lenticulars (S0), Spirals (Sp) and Irregulars (I). We have compared our classification with that reported by Fasano et al. (2000) for the galaxies in common. In Fig. 5, we show the result of that comparison. 70% of the galaxies were classified as the same type, whereas 20% differ by only one type. The morphological classification for that bright subsample is given in the last column of the table in the appendix.

In Table 4, we show the percentages of the different galaxy types in the central part of each cluster in the 420 and 735 kpc aperture respectively. Notice that A1643 and A1878 have a large number of late type galaxies (about 60%). In particular, A1878 also contains a large fraction of irregular galaxies (19%). The rest of the clusters have an early-type population dominating in their cores. A diversity is clear as far as morphological populations is concerned.

5.1. Morphological distribution of the galaxies in the clusters

It is well known that early-type galaxies in clusters at low redshift are in general located in denser regions and closer to the center of the cluster than later types, (Dressler 1980). We want now to investigate the way in which those clusters at medium redshift are populated.

In Fig. 6, we have plotted the cumulative functions of the different types of galaxies versus projected distance of each galaxy to the center of the cluster. The solid lines represent the cumulative distribution of early-type, elliptical and lenticular, galaxies; the dotted lines correspond to the cumulative distribution of late-type galaxies, spiral and irregular. The vertical lines indicate the radius where the cumulative distributions reach 50% of the distributions.

We see that all the clusters are dominated in their central regions by early type galaxies except A1878, that has a sizable fraction of late-type, including irregular galaxies, which may explain its high (central) fraction of blue galaxies. However, this is not unique since similar cases can also be found at lower redshift (see for example Varela 2004). A1643 has also a large global fraction of late-type, spiral galaxies, but they do not dominate the core of the cluster. The rest of the clusters are also centrally dominated by a population of elliptical galaxies, with an overall population with a smaller fraction of late-type galaxies. As we noticed before, diversity seems to be the dominant aspect of our five clusters.

To test whether the distribution of early and late type galaxies are similar, we have performed a Kolmogorov-Smirnov test. Excluding A2658, for which there are not enough points to extract significant results, we find that the two populations are significantly different in two clusters, A1878 and A1952, while for

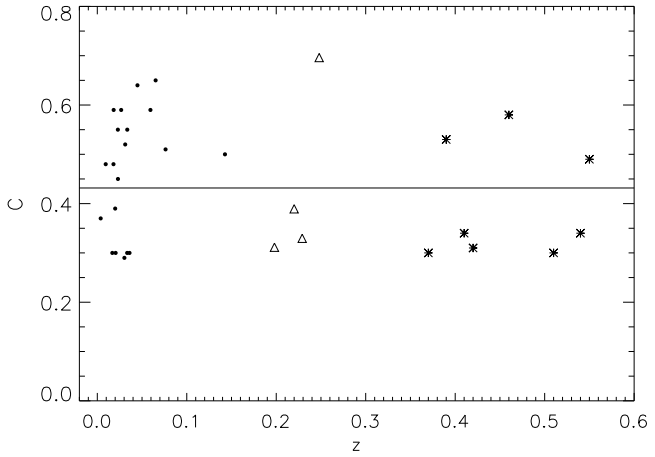

Fig. 7. Concentration parameter versus redshift for our clusters (triangles), a low-redshift compilation (Butcher & Oemler 1978: black points) and a higher redshift sample (Dressler et al. 1997: asteriks). The horizontal line is the mean concentration value of the clusters with enough area coverage.

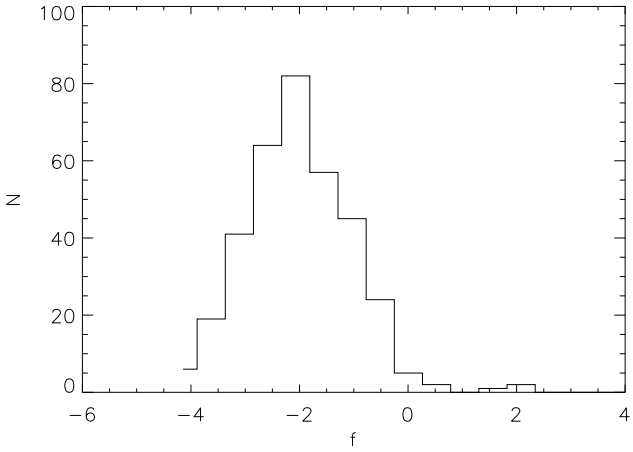

Fig. 8. Histogram of the f-parameter values for the galaxies belonging to our clusters.

the other two, A1643 and A2111, the KS test does not allow us to extract significant results. Then, A1878 and A1952 show morphological segregation as found in low redshift samples such as, by Adami et al. (1998). Moreover, in the case of A1878 the dominant morphological population is late type galaxies.

5.2. The concentration parameter

We have calculated the concentration parameter of our clusters in the central 735 kpc using the definition given by Butcher & Oemler (1978), $\log(R_{60}/R_{20})$, where R_{60} and R_{20} are the radii containing 60% and 20% of the cluster populations within 735 kpc. Only the four clusters with enough area coverage were analyzed. The concentration values we have found are 0.311 for A1643, 0.389 for A1878, 0.329 for A2111 and 0.696 for A1952 as can be seen in Fig. 7. We have overplotted the values found for lower z clusters by Butcher & Oemler (1978) and for a higher redshift sample by Dressler et al. (1997). As can be seen in the figure, our concentration values span the full range of the values measured for lower redshfit clusters. Moreover, this range encompasses also that of the higher redshift cluster concentration values. It does not seem, therefore, that there is any clear tendency of the change in concentration parameter with redshift or morphological type. At most, it could be argued that clusters tend to progressively populate the lower half of the plane when the redshift increases.

Likewise, Butcher & Oemler (1978) and Dressler et al. (1997) suggested that the more irregular, less concentrated clusters would be preferentially populated by late type galaxies. In that sense, we notice that A1643, the cluster with the largest global fraction of late-type galaxies, presents the lowest value of the concentration parameter. Moreover, A1878, another cluster with a low concentration index also presents a rather high fraction of late type and irregular galaxies and, is dominated by this population. However, A2111, our third cluster with a low concentration, is dominated by an early-type population. Thus, although there is an indication of a higher fraction of irregular clusters with increasing redshift, the small statistics prevent us from reaching a firm conclusion.

5.3. Interaction systems

Another interesting feature for consideration in clusters at that range of redshift is the proportion of interacting systems compared to lower redshift clusters. To investigate this, we have calculated the distribution of the f-parameter defined by Varela et al. (2004) for the galaxies in the final catalogue. It gives an account of the relative importance of the tidal forces for each galaxy. Larger values indicate a larger proportion of interaction systems. The result is plotted in Fig. 8. The median value of the distribution is −1.59, whereas the median value found for the Coma Cluster is −2.7 (Varela et al. 2004). Moreover, we find that 63.97% of the galaxies have a perturbation parameter higher than −2, which is the value chosen by Varela et al. (2004) to select truly interacting systems.

More specifically, the median f-values we find are −1.39 (A2658), −1.92 (A1643), −1.60 (A1878), −1.67 (A2111) and −1.29 (A1952), all of them larger than −2. This is indicative of the presence of a larger population of interacting systems in our sample than in the Coma Cluster.

6. Discussion and conclusions

It is well known that locally, the color−magnitude relation for early-type galaxies has a well-defined slope with a small scatter, (Bower et al. 1992). Results based on HST data (Ellis et al. 1997; Stanford et al. 1998; Mei et al. 2006) demonstrated the existence of a tight red sequence in clusters at redshift up to 1.26, comparable in scatter and slope to that observed in the Coma Cluster and low redshift clusters. In agreement with these results, we find no significant difference in the slope of the CMR for our cluster sample and other samples at different redshift values. This reinforces the conclusion of the universality of the CMR on all the explored z-range.

Regarding the Butcher-Oemler effect, the values we obtain for the blue galaxy fraction are similar to those found by De Propris et al. (2004) for lower redshift SDSS clusters. The only outstanding case in our sample is A1878, with a large blue fraction. This goes together with a large fraction of late type and irregular galaxies in its central region and a low value of the concentration parameter. However, this case is not unique, (see for example, De Propris et al. 2004; Aguerri et al. 2007). The blue fraction values that we find indicate that there is no evolution in this parameter at least up to redshift 0.25. Thus, the

Butcher-Oemler effect starts to manifest at even higher redshift. This is in agreement with previous results obtained with other samples (see Andreon et al. 2006). That conclusion, together with the universality of the CMR suggests that the stellar population in cluster galaxies has not evolved significantly in the last 2.5 Gyr.

We have found differences in the fraction of blue galaxies with the aperture considered for its determination, in the sense indicated by other reported results (Margoniner & de Carvalho 2000; Goto et al. 2003; De Propris et al. 2004), and in agreement with other values found in the literature for the blue fraction of A2111. However, these differences are not significant.

The morphological segregation between early and late-type galaxies observed in nearby clusters (Adami et al. 1998; Aguerri et al. 2004) has been shown to be present in two clusters from our medium reshift sample. However, the range of situations we find is similar to that found at lower redshift and no evolutionary trend is manifested through it.

We have also looked at the degree of interaction of the galaxies in our sample. We have found that the median value of the f-parameter is significantly higher than in the Coma cluster in all our five clusters. A wider sample at low redshift is lacking to enable us to draw conclusions about the possible higher incidence of interactions at higher redshift.

The results we have obtained suggest that the evolutionary status of clusters at $z \sim 0.2$ is not significantly different from that of clusters at lower redshift. Indeed, larger samples at intermediate redshifts are needed to establish whether the trends with z indicated by the concentration parameter are real or only artifacts produced by the small size of the available samples.

On the other hand, some parameters like the CMR slope are remarkably constant with redshift, strongly supporting the view that the red sequence was well established soon after the formation of the red, bright cluster galaxies. Regarding the Butcher-Oemler effect our results reinforce the view that it starts to appear at rather high z-values, larger than $z \sim 0.25$. As far as the morphological mixing is concerned, the values span a wide range, similarly to other samples at lower or higher redshift, indicating that here also diversity is the dominant aspect.

Acknowledgements. We acknowledge the anonymous referee for useful comments and suggestions. Begoña Ascaso is supported by an I3P Individual Fellowship from the Consejo Superior de Investigaciones Cientificas at the Instituto de Astrofísica de Andalucía. J.A.L.A. acknowledges finalcial support by the project ESTALLIDOS AYA2007-67965-C03-01. We also acknowledge a grant by the Spanish Ministerio de Educacion y Ciencia, reference PNAYA2006-14056 and Proyecto de Excelencia of the Junta de Andalucia, reference J.A FQM 1392.

References

Abell, G. O., Corwin, H. G., Jr., & Olowin, R. P. 1989, ApJS, 70, 1
Adami, C., Biviano, A., & Mazure, A. 1998, A&A, 331, 439
Aguerri, J. A. L., Balcells, M., & Peletier, R. F. 2001, A&A, 367, 428
Aguerri, J. A. L., Iglesias-Paramo, J., Vilchez, J. M., & Muñoz-Tuñón, C. 2004, AJ, 127, 134
Aguerri, J. A. L., Sánchez-Janssen, R., & Muñoz-Tuñón, C. 2007, A&A, 471, 17
Andreon, S., Quintana, H., Tajer, M., Galaz, G., & Surdej, J. 2006, MNRAS, 365, 915
Armstrong, R. D., & Kung, M. T. 1978, Appl. Stat., 27, 363
Babu, G. J., & Singh, K. 1983, Ann. Stat., 11, 999
Baum, W. A. 1959, PASP, 71, 106
Bekki, K., Couch, W. J., & Shioya, Y. 2002, ApJ, 577, 651
Bertin, E., & Arnouts, S. 1996, A&AS, 117, 393
Bower, R. G., Lucey, J. R., & Ellis, R. S. 1992, MNRAS, 254, 589
Bower, R. G., Kodama, T., & Terlevich, A. 1998, MNRAS, 299, 1193
Butcher, H., & Oemler, A., Jr. 1978, ApJ, 226, 559
Butcher, H., & Oemler, A., Jr. 1984, ApJ, 285, 426
de Jong, R. S. 1996, A&AS, 118, 557
De Lucia, G., & Blaizot, J. 2007, MNRAS, 375, 2
De Lucia, G., Poggianti, B. M., Arago'n-Salamanca, A., et al. 2007, MNRAS, 374, 809
De Propris, R., Colless, M., Peacock, J. A., et al. 2004, MNRAS, 351, 125
Dressler, A. 1980, ApJ, 236, 351
Dressler, A., Oemler, A., Jr., Couch, W. J., et al. 1997, ApJ, 490, 577
Driver, S. P., Allen, P. D., Graham, A. W., et al. 2006, MNRAS, 368, 414
Efron, B., & Tibshirani, R. 1986, Stat. Sci., 1, 54
Eliche-Moral, M. C., Balcells, M., Aguerri, J. A. L., & González-García, A. C. 2006, A&A, 457, 91
Ellis, R. S., Smail, I., Dressler, A., et al. 1997, ApJ, 483, 582
Fasano, G., Poggianti, B. M., Couch, W. J., et al. 2000, ApJ, 542, 673
Fasano, G., Bettoni, D., D'Onofrio, M., Kjærgaard, P., & Moles, M. 2002, A&A, 387, 26
Fetisova, T. S., 1982, SvA, 25, 647
Gal, R. R., de Carvalho, R. R., Lopes, P. A. A., et al. 2003, AJ, 125, 2064
Gerhard, O. E., & Fall, S. M. 1983, MNRAS, 203, 1253
Goto, T., Okamura, S., Yagi, M., et al. 2003, PASJ, 55, 739
Graham, A. W., & de Blok, W. J. G. 2001, ApJ, 556, 177
Graham, A. W., & Guzmán, R. 2003, AJ, 125, 2936
Gunn, J. E., & Gott, J. R. I. 1972, ApJ, 176, 1
Henriksen, M., Wang, Q. D., & Ulmer, M. 1999, MNRAS, 307, 67
Humason, M. L., Mayall, N. U., & Sandage, A. R. 1956, AJ, 61, 97
Jorgensen, I. 1994, PASP, 106, 967
Jorgensen, I., Franx, M., & Kjaergaard, P. 1992, A&AS, 95, 489
Kauffmann, G., Guiderdoni, B., & White, S. D. M. 1994, MNRAS, 267, 981
Kodama, T. 1999, Star Formation in Early Type Galaxies, 163, 250
Landolt, A. U. 1992, AJ, 104, 340
Lavery, R. J., & Henry, J. P. 1986, ApJ, 304, L5
López-Cruz, O., Barkhouse, W. A., & Yee, H. K. C. 2004, ApJ, 614, 679
Margoniner, V. E., & de Carvalho, R. R. 2000, AJ, 119, 1562
Mei, S., Holden, B. P., Blakeslee, J. P., et al. 2006, ApJ, 644, 759
Merritt, D. 1984, ApJ, 276, 26
Miller, N. A., Oegerle, W. R., & Hill, J. M. 2006, AJ, 131, 2426
Montgomery, K. A., Marschall, L. A., & Janes, K. A. 1993, AJ, 106, 181
Moore, B., Katz, N., Lake, G., Dressler, A., & Oemler, A. 1996, Nature, 379, 613
Nelson, A. E., Gonzalez, A. H., Zaritsky, D., & Dalcanton, J. J. 2002, ApJ, 566, 103
Pence, W. 1976, ApJ, 203, 39
Quilis, V., Moore, B., & Bower, R. 2000, Science, 288, 1617
Rood, H. J. 1969, ApJ, 158, 657
Sandage, A., Kristian, J., & Westphal, J. A. 1976, ApJ, 205, 688
Stanford, S. A., Eisenhardt, P. R., & Dickinson, M. 1998, ApJ, 492, 461
Stott, J. P., Edge, A. C., Smith, G. P., Swinbank, A. M., & Ebeling, H. 2008, MNRAS, 384, 1502
Trujillo, I., Aguerri, J. A. L., Gutiérrez, C. M., & Cepa, J. 2001, AJ, 122, 38
Varela, J., 2004, Ph.D. Thesis, Computense University of Madrid
Varela, J., Moles, M., Márquez, I., et al. 2004, A&A, 420, 873
Visvanathan, N., & Griersmith, D. 1977, A&A, 59, 317
Visvanathan, N., & Sandage, A. 1977, ApJ, 216, 214
Wang, Q. D., Ulmer, M. P., & Lavery, R. J. 1997, MNRAS, 288, 702

Appendix A: Catalogue of galaxies detected in the cluster sample

Name	α (J2000)			δ (J2000)			z	M_r	M_B	Morph
A 2658	23h	44m	47.99s	–12d	18m	46.20s		–19.12	–18.24	
A 2658	23h	44m	55.21s	–12d	18m	37.00s		–18.98	–18.20	
A 2658	23h	44m	49.55s	–12d	18m	34.40s		–19.65	–18.99	
A 2658	23h	44m	49.62s	–12d	18m	31.90s		–18.68	–18.01	
A 2658	23h	44m	50.35s	–12d	18m	25.50s		–21.89	–21.06	S
A 2658	23h	44m	49.13s	–12d	18m	19.80s		–19.29	–18.34	
A 2658	23h	44m	47.27s	–12d	18m	13.40s		–19.24	–19.14	
A 2658	23h	44m	46.97s	–12d	18m	10.40s		–20.94	–20.12	S0
A 2658	23h	44m	49.36s	–12d	18m	07.90s		–18.44	–17.53	
A 2658	23h	44m	52.22s	–12d	18m	04.60s		–19.99	–18.90	E
A 2658	23h	44m	54.99s	–12d	18m	05.60s		–18.08	–17.23	
A 2658	23h	44m	54.27s	–12d	17m	59.30s		–21.42	–20.39	E
A 2658	23h	44m	50.42s	–12d	17m	56.40s		–19.39	–18.41	
A 2658	23h	44m	51.64s	–12d	17m	53.30s		–18.71	–18.11	
A 2658	23h	44m	47.44s	–12d	17m	47.40s		–20.92	–19.87	E
A 2658	23h	44m	50.34s	–12d	17m	32.70s		–18.84	–20.30	
A 2658	23h	44m	49.28s	–12d	17m	38.20s		–18.19	–19.65	
A 2658	23h	44m	50.26s	–12d	17m	20.90s		–21.07	–20.35	S0
A 2658	23h	44m	49.84s	–12d	17m	26.70s		–21.32	–20.95	E
A 2658	23h	44m	49.80s	–12d	17m	39.50s		–22.39	–22.02	E
A 2658	23h	44m	54.96s	–12d	17m	38.80s		–18.80	–18.35	
A 2658	23h	44m	55.87s	–12d	17m	37.60s		–18.22	–17.40	
A 2658	23h	44m	51.86s	–12d	17m	35.30s		–19.57	–18.55	
A 2658	23h	44m	47.85s	–12d	17m	31.10s		–18.14	–17.23	
A 2658	23h	44m	50.96s	–12d	17m	19.10s		–20.24	–19.17	E
A 2658	23h	44m	55.84s	–12d	17m	17.60s		–20.18	–19.15	S0
A 2658	23h	44m	51.40s	–12d	17m	11.00s		–18.35	–18.28	
A 2658	23h	44m	56.18s	–12d	17m	07.50s		–21.14	–20.31	S
A 2658	23h	44m	51.13s	–12d	16m	48.00s		–20.61	–19.49	E
A 2658	23h	44m	46.13s	–12d	16m	49.10s		–18.82	–18.35	
A 2658	23h	44m	49.65s	–12d	16m	35.80s		–20.56	–19.43	S0
A 2658	23h	44m	47.99s	–12d	16m	36.20s		–18.29	–17.66	
A 2658	23h	44m	51.63s	–12d	16m	28.80s		–18.70	–17.79	
A 2658	23h	44m	53.27s	–12d	16m	23.60s		–18.27	–17.77	
A 1643	12h	55m	52.30s	44d	05m	47.30s		–19.88	–20.46	S
A 1643	12h	55m	52.44s	44d	05m	52.70s		–19.52	–20.82	
A 1643	12h	55m	54.14s	44d	05m	52.70s		–19.79	–18.64	
A 1643	12h	55m	59.31s	44d	05m	53.20s		–19.36	–17.98	
A 1643	12h	55m	53.80s	44d	03m	15.20s		–19.79	–18.61	S
A 1643	12h	55m	55.18s	44d	03m	47.50s		–20.67	–19.46	S0
A 1643	12h	55m	49.83s	44d	04m	08.80s		–19.82	–19.24	
A 1643	12h	55m	49.75s	44d	04m	05.50s		–20.61	–19.63	S
A 1643	12h	55m	47.93s	44d	04m	01.20s		–20.36	–19.10	E
A 1643	12h	55m	48.06s	44d	04m	06.70s		–18.24	–17.09	
A 1643	12h	55m	51.98s	44d	04m	05.90s		–18.93	–19.06	
A 1643	12h	55m	59.67s	44d	04m	05.20s		–19.64	–18.62	S
A 1643	12h	55m	53.06s	44d	04m	06.60s		–18.89	–17.82	
A 1643	12h	55m	55.75s	44d	04m	07.30s		–19.39	–18.88	
A 1643	12h	56m	01.43s	44d	04m	07.90s		–19.71	–19.19	
A 1643	12h	55m	53.64s	44d	04m	13.70s		–20.09	–19.36	S
A 1643	12h	55m	50.96s	44d	04m	31.00s		–21.15	–20.05	E
A 1643	12h	55m	59.04s	44d	04m	26.90s		–19.00	–17.81	
A 1643	12h	55m	55.35s	44d	04m	34.40s		–20.69	–20.35	E
A 1643	12h	55m	54.88s	44d	04m	33.90s		–20.14	–19.56	S
A 1643	12h	55m	56.61s	44d	04m	38.20s		–18.70	–20.14	
A 1643	12h	55m	52.33s	44d	04m	46.80s		–18.42	–19.14	
A 1643	12h	55m	52.97s	44d	04m	50.00s		–19.82	–19.09	
A 1643	12h	55m	52.96s	44d	04m	39.20s	0.1978	–19.73	–19.60	S
A 1643	12h	55m	52.70s	44d	04m	44.50s		–20.42	–19.74	S0
A 1643	12h	55m	54.94s	44d	04m	45.60s		–19.29	–19.15	
A 1643	12h	55m	48.16s	44d	04m	49.50s		–19.49	–18.74	
A 1643	12h	55m	47.94s	44d	04m	51.60s		–19.59	–18.95	
A 1643	12h	55m	51.98s	44d	04m	53.10s		–19.57	–19.08	
A 1643	12h	55m	55.21s	44d	04m	53.10s		–18.00	–17.50	
A 1643	12h	55m	54.40s	44d	04m	53.70s		–18.26	–17.50	
A 1643	12h	55m	59.29s	44d	04m	57.10s		–20.02	–18.94	S

Table A.1. continued.

Name	α (J2000)			δ (J2000)			z	M_r	M_B	Morph
A 1643	12h	55m	56.07s	44d	04m	58.00s		–18.49	–17.59	
A 1643	12h	55m	54.00s	44d	05m	12.40s		–21.61	–20.35	S0
A 1643	12h	56m	01.63s	44d	05m	09.10s		–19.45	–18.11	
A 1643	12h	55m	49.61s	44d	05m	09.50s		–18.25	–17.15	
A 1643	12h	55m	47.67s	44d	05m	15.70s		–18.15	–17.15	
A 1643	12h	55m	54.61s	44d	05m	21.40s		–19.23	–17.99	
A 1643	12h	55m	53.05s	44d	05m	23.40s		–20.19	–18.97	S0
A 1643	12h	56m	00.41s	44d	05m	29.90s		–19.20	–18.91	
A 1643	12h	55m	48.02s	44d	05m	35.90s		–19.73	–18.91	
A 1643	12h	55m	52.36s	44d	05m	38.40s		–19.16	–19.35	
A 1643	12h	55m	52.76s	44d	05m	37.90s		–19.88	–19.97	S
A 1643	12h	55m	54.21s	44d	05m	44.70s		–19.41	–18.29	
A 1643	12h	56m	01.53s	44d	03m	29.90s		–18.65	–20.27	
A 1643	12h	55m	50.27s	44d	03m	30.50s		–19.27	–18.68	
A 1643	12h	55m	53.07s	44d	05m	47.80s		–18.67	–17.64	
A 1643	12h	55m	48.08s	44d	05m	51.70s		–18.23	–17.80	
A 1643	12h	55m	34.43s	44d	08m	50.30s		–19.53	–18.37	
A 1643	12h	55m	44.49s	44d	08m	53.60s		–19.09	–18.13	
A 1643	12h	55m	45.49s	44d	06m	39.60s		–18.15	–19.35	
A 1643	12h	55m	44.70s	44d	06m	35.60s		–19.65	–18.94	
A 1643	12h	55m	38.43s	44d	06m	29.90s		–18.50	–17.72	
A 1643	12h	55m	38.94s	44d	06m	35.20s		–18.31	–17.92	
A 1643	12h	55m	45.18s	44d	06m	46.30s		–19.68	–18.40	E
A 1643	12h	55m	32.98s	44d	06m	50.40s		–19.92	–19.46	S
A 1643	12h	55m	33.62s	44d	06m	30.00s		–18.06	–17.72	
A 1643	12h	55m	37.87s	44d	06m	57.10s		–18.59	–17.40	
A 1643	12h	55m	46.43s	44d	06m	58.80s		–18.14	–17.06	
A 1643	12h	55m	33.82s	44d	07m	12.50s		–20.93	–19.67	E
A 1643	12h	55m	36.30s	44d	07m	15.70s		–18.80	–18.47	
A 1643	12h	55m	41.25s	44d	07m	15.00s		–18.32	–17.59	
A 1643	12h	55m	39.33s	44d	07m	21.30s		–19.72	–18.39	S
A 1643	12h	55m	37.74s	44d	07m	23.30s		–18.00	–17.63	
A 1643	12h	55m	38.60s	44d	07m	29.10s		–18.09	–16.93	
A 1643	12h	55m	46.75s	44d	07m	35.40s		–18.99	–17.90	
A 1643	12h	55m	42.78s	44d	07m	48.60s		–18.24	–16.93	
A 1643	12h	55m	36.40s	44d	07m	53.40s		–20.71	–20.57	I
A 1643	12h	55m	36.55s	44d	07m	54.10s		–20.34	–20.10	
A 1643	12h	55m	36.63s	44d	08m	20.30s		–20.17	–20.49	I
A 1643	12h	55m	36.38s	44d	08m	24.40s		–19.77	–19.13	S0
A 1643	12h	55m	36.57s	44d	08m	30.40s		–20.27	–19.84	E
A 1643	12h	55m	43.31s	44d	08m	28.90s		–18.20	–18.04	
A 1643	12h	55m	38.31s	44d	08m	38.70s		–18.02	–17.76	
A 1643	12h	55m	37.59s	44d	06m	21.10s		–19.42	–18.66	S
A 1878	14h	12m	54.12s	29d	16m	16.60s		–18.74	–17.61	
A 1878	14h	12m	49.83s	29d	13m	40.60s		–18.90	–18.43	
A 1878	14h	12m	47.43s	29d	13m	55.50s		–18.53	–20.39	
A 1878	14h	12m	47.82s	29d	13m	53.40s		–21.69	–20.68	S
A 1878	14h	12m	53.32s	29d	13m	47.00s		–18.37	–18.29	
A 1878	14h	12m	54.23s	29d	13m	57.60s		–20.23	–20.50	S
A 1878	14h	12m	50.11s	29d	13m	59.90s		–18.63	–19.32	
A 1878	14h	12m	49.97s	29d	14m	02.60s		–20.45	–19.30	S
A 1878	14h	12m	56.80s	29d	14m	03.60s		–20.38	–20.06	I
A 1878	14h	12m	54.78s	29d	14m	03.90s		–18.55	–17.39	
A 1878	14h	12m	47.17s	29d	14m	05.80s		–20.04	–19.70	I
A 1878	14h	12m	49.47s	29d	14m	09.90s		–21.57	–20.53	S
A 1878	14h	12m	49.03s	29d	14m	07.80s		–18.94	–21.00	
A 1878	14h	12m	52.50s	29d	14m	11.40s		–20.94	–20.28	S
A 1878	14h	12m	54.85s	29d	14m	17.30s		–19.91	–19.67	S
A 1878	14h	12m	54.65s	29d	14m	23.80s		–19.23	–19.19	
A 1878	14h	12m	47.85s	29d	14m	17.10s		–19.70	–18.95	
A 1878	14h	12m	54.15s	29d	14m	19.30s		–20.80	–19.49	E
A 1878	14h	12m	52.75s	29d	14m	20.20s		–18.72	–20.18	
A 1878	14h	12m	52.18s	29d	14m	28.40s	0.2220	–22.36	–21.69	E
A 1878	14h	12m	46.85s	29d	14m	26.40s		–21.02	–20.50	I
A 1878	14h	12m	54.72s	29d	14m	31.90s		–21.42	–20.23	E
A 1878	14h	12m	56.29s	29d	14m	31.40s		–20.24	–19.80	I
A 1878	14h	12m	51.24s	29d	14m	48.20s		–20.10	–20.01	S

Table A.1. continued.

Name	α (J2000)			δ (J2000)			z	M_r	M_B	Morph
A 1878	14h	12m	51.04s	29d	14m	39.30s		–19.72	–20.22	
A 1878	14h	12m	50.98s	29d	14m	42.30s		–20.84	–21.55	I
A 1878	14h	12m	46.74s	29d	14m	40.00s		–18.44	–18.10	
A 1878	14h	12m	53.29s	29d	14m	41.40s		–20.30	–20.22	
A 1878	14h	12m	53.32s	29d	14m	44.60s		–19.55	–21.50	
A 1878	14h	12m	49.12s	29d	14m	42.50s		–21.38	–20.33	S
A 1878	14h	12m	50.12s	29d	14m	47.30s		–20.40	–19.13	S0
A 1878	14h	12m	52.25s	29d	14m	53.70s		–20.41	–20.57	S
A 1878	14h	12m	51.99s	29d	14m	57.10s		–19.53	–19.92	
A 1878	14h	12m	50.96s	29d	14m	56.60s		–21.29	–20.33	S
A 1878	14h	12m	46.14s	29d	14m	55.60s		–19.94	–19.35	S0
A 1878	14h	12m	46.58s	29d	14m	59.10s		–20.94	–19.69	S0
A 1878	14h	12m	53.29s	29d	14m	56.90s		–18.53	–17.55	
A 1878	14h	12m	48.23s	29d	15m	01.10s		–19.28	–18.27	
A 1878	14h	12m	50.01s	29d	15m	05.00s		–18.23	–17.10	
A 1878	14h	12m	56.61s	29d	15m	05.30s		–19.18	–19.30	
A 1878	14h	12m	49.37s	29d	15m	12.10s		–18.79	–17.72	
A 1878	14h	12m	50.60s	29d	15m	13.20s		–18.64	–18.42	
A 1878	14h	12m	49.68s	29d	15m	14.20s		–19.56	–19.22	
A 1878	14h	12m	55.12s	29d	15m	14.70s		–18.85	–17.83	
A 1878	14h	12m	51.24s	29d	15m	22.10s		–19.89	–19.95	S
A 1878	14h	12m	53.39s	29d	15m	22.30s		–19.01	–18.65	
A 1878	14h	12m	51.04s	29d	15m	28.90s		–19.51	–21.46	
A 1878	14h	12m	53.49s	29d	15m	27.70s		–18.76	–18.14	
A 1878	14h	12m	52.60s	29d	15m	41.10s		–18.61	–18.01	
A 1878	14h	12m	52.43s	29d	15m	48.70s		–21.00	–19.79	S0
A 1878	14h	12m	55.73s	29d	15m	56.70s		–18.18	–17.32	
A 1878	14h	12m	53.61s	29d	16m	00.80s		–19.77	–18.60	
A 1878	14h	12m	53.04s	29d	16m	07.40s		–18.86	–21.15	
A 1878	14h	12m	47.96s	29d	16m	09.50s		–19.69	–19.16	
A 1878	14h	13m	00.54s	29d	13m	56.90s		–21.15	–20.41	S0
A 1878	14h	12m	56.76s	29d	14m	03.60s		–20.00	–20.14	I
A 1878	14h	12m	56.78s	29d	12m	00.30s		–19.87	–18.86	S0
A 1878	14h	12m	57.80s	29d	12m	01.60s		–20.47	–19.97	S0
A 1878	14h	12m	59.05s	29d	12m	14.40s		–20.60	–20.01	E
A 1878	14h	12m	59.84s	29d	12m	19.50s		–20.45	–21.96	S
A 1878	14h	13m	00.58s	29d	12m	22.90s		–20.30	–19.90	S
A 1878	14h	13m	01.89s	29d	12m	17.50s		–19.55	–18.93	S
A 1878	14h	13m	05.79s	29d	12m	20.80s		–18.24	–18.48	
A 1878	14h	12m	58.97s	29d	12m	33.00s		–18.13	–17.07	
A 1878	14h	13m	01.29s	29d	12m	36.90s		–20.97	–20.65	S0
A 1878	14h	13m	05.52s	29d	12m	36.60s		–18.59	–18.07	
A 1878	14h	13m	02.23s	29d	12m	40.50s		–18.23	–18.12	
A 1878	14h	13m	05.38s	29d	12m	42.80s		–18.24	–17.75	
A 1878	14h	12m	58.42s	29d	12m	53.60s		–18.05	–19.13	
A 1878	14h	12m	58.26s	29d	12m	54.90s		–19.49	–20.04	
A 1878	14h	13m	05.59s	29d	12m	54.20s		–20.53	–19.81	E
A 1878	14h	13m	04.82s	29d	12m	55.40s		–19.03	–18.41	
A 1878	14h	13m	02.81s	29d	12m	55.70s		–19.44	–18.73	S
A 1878	14h	12m	58.70s	29d	12m	56.60s		–18.92	–18.15	
A 1878	14h	13m	04.41s	29d	13m	00.70s		–20.06	–19.78	S
A 1878	14h	12m	55.45s	29d	13m	04.30s		–19.48	–19.63	I
A 1878	14h	12m	55.11s	29d	13m	09.90s		–19.13	–19.64	
A 1878	14h	12m	57.07s	29d	13m	19.80s		–18.08	–18.08	
A 1878	14h	12m	57.65s	29d	13m	22.20s		–18.09	–17.93	
A 1878	14h	13m	00.40s	29d	13m	37.50s		–19.13	–18.71	
A 1878	14h	12m	57.01s	29d	13m	43.90s		–19.27	–18.62	
A 1878	14h	12m	57.70s	29d	13m	48.90s		–19.78	–19.18	S0
A 1878	14h	13m	03.99s	29d	13m	53.50s		–19.36	–19.74	
A 1878	14h	13m	02.65s	29d	14m	01.20s		–18.08	–18.25	
A 2111	15h	39m	35.52s	34d	26m	56.20s		–20.46	–19.56	S
A 2111	15h	39m	37.64s	34d	27m	03.80s	0.2295	–21.26	–20.22	S0
A 2111	15h	39m	31.84s	34d	27m	05.10s		–19.01	–18.09	
A 2111	15h	39m	38.48s	34d	24m	32.40s		–19.37	–18.96	
A 2111	15h	39m	40.16s	34d	24m	18.10s		–19.38	–18.33	
A 2111	15h	39m	39.34s	34d	24m	44.50s		–20.26	–19.31	E
A 2111	15h	39m	38.45s	34d	24m	51.40s		–20.02	–19.08	

Table A.1. continued.

Name	α (J2000)			δ (J2000)			z	M_r	M_B	Morph
A 2111	15h	39m	40.16s	34d	24m	55.70s		–20.49	–19.27	S0
A 2111	15h	39m	42.76s	34d	24m	56.60s		–18.32	–17.38	
A 2111	15h	39m	37.84s	34d	24m	57.00s		–18.55	–17.54	
A 2111	15h	39m	39.81s	34d	25m	00.50s		–18.06	–17.79	
A 2111	15h	39m	37.21s	34d	25m	08.50s		–19.67	–18.70	S
A 2111	15h	39m	40.49s	34d	25m	27.30s	0.2282	–22.67	–21.51	E
A 2111	15h	39m	39.75s	34d	25m	23.10s		–19.57	–18.85	
A 2111	15h	39m	39.20s	34d	25m	11.50s		–21.13	–20.38	E
A 2111	15h	39m	39.39s	34d	25m	13.40s	0.2211	–21.34	–20.61	E
A 2111	15h	39m	36.23s	34d	25m	12.10s		–20.34	–19.21	S0
A 2111	15h	39m	34.90s	34d	25m	14.50s		–18.97	–18.02	
A 2111	15h	39m	40.27s	34d	25m	34.80s		–20.07	–21.06	
A 2111	15h	39m	38.15s	34d	25m	18.10s		–20.21	–19.01	S0
A 2111	15h	39m	37.53s	34d	25m	18.70s		–19.62	–18.72	S
A 2111	15h	39m	36.64s	34d	25m	29.00s		–18.96	–18.34	
A 2111	15h	39m	33.61s	34d	25m	34.00s		–18.48	–17.78	
A 2111	15h	39m	36.79s	34d	25m	39.10s	0.2312	–20.90	–19.65	S0
A 2111	15h	39m	39.69s	34d	25m	21.20s		–20.40	–19.70	
A 2111	15h	39m	31.27s	34d	25m	40.00s		–20.24	–19.65	
A 2111	15h	39m	38.68s	34d	25m	38.90s		–18.16	–17.04	
A 2111	15h	39m	37.29s	34d	25m	45.90s		–18.49	–17.33	
A 2111	15h	39m	36.42s	34d	25m	50.10s		–20.46	–19.50	E
A 2111	15h	39m	41.20s	34d	25m	50.90s		–20.53	–19.36	S0
A 2111	15h	39m	40.18s	34d	25m	50.80s		–18.60	–17.90	
A 2111	15h	39m	33.99s	34d	25m	51.30s		–19.30	–18.23	
A 2111	15h	39m	37.44s	34d	25m	54.80s		–20.12	–18.98	E
A 2111	15h	39m	39.52s	34d	25m	56.90s		–19.23	–18.23	
A 2111	15h	39m	39.91s	34d	25m	57.20s		–18.53	–17.69	
A 2111	15h	39m	41.69s	34d	26m	01.70s		–18.03	–16.89	
A 2111	15h	39m	31.72s	34d	26m	07.20s		–20.49	–19.37	S0
A 2111	15h	39m	36.84s	34d	26m	07.20s		–20.44	–19.68	I
A 2111	15h	39m	38.07s	34d	26m	09.50s		–18.64	–19.00	
A 2111	15h	39m	34.11s	34d	26m	19.20s		–20.80	–20.58	S
A 2111	15h	39m	34.26s	34d	26m	12.50s	0.2289	–21.97	–21.11	S0
A 2111	15h	39m	38.18s	34d	26m	06.90s		–19.72	–19.53	
A 2111	15h	39m	32.26s	34d	26m	12.80s		–19.25	–18.22	
A 2111	15h	39m	38.58s	34d	26m	28.20s		–20.23	–19.24	S
A 2111	15h	39m	39.03s	34d	26m	38.10s		–19.29	–19.48	
A 2111	15h	39m	38.70s	34d	26m	38.80s	0.2246	–20.85	–20.29	S
A 2111	15h	39m	37.81s	34d	26m	35.90s		–18.12	–17.73	
A 2111	15h	39m	31.99s	34d	26m	36.10s		–18.39	–18.00	
A 2111	15h	39m	35.47s	34d	26m	43.70s		–20.70	–19.87	S0
A 2111	15h	39m	41.19s	34d	26m	41.30s		–20.27	–20.24	I
A 2111	15h	39m	40.90s	34d	26m	45.40s		–19.28	–19.45	
A 2111	15h	39m	37.59s	34d	26m	44.20s		–18.92	–18.91	
A 2111	15h	39m	33.13s	34d	26m	45.60s		–19.25	–18.91	
A 2111	15h	39m	37.16s	34d	26m	45.70s		–18.26	–17.93	
A 2111	15h	39m	38.38s	34d	26m	50.50s		–18.01	–17.13	
A 2111	15h	39m	32.78s	34d	24m	22.40s		–19.21	–18.31	
A 2111	15h	39m	41.34s	34d	24m	34.30s	0.2294	–20.97	–20.81	S
A 2111	15h	39m	41.81s	34d	24m	42.70s	0.2292	–22.61	–22.18	E
A 2111	15h	39m	42.27s	34d	24m	40.40s		–19.08	–20.81	
A 2111	15h	39m	41.26s	34d	24m	43.60s		–20.43	–22.04	S
A 2111	15h	39m	47.09s	34d	27m	37.90s	0.2368	–21.25	–20.57	S0
A 2111	15h	39m	42.81s	34d	27m	44.60s		–19.68	–19.55	I
A 2111	15h	39m	52.99s	34d	27m	48.60s	0.2297	–20.98	–19.94	S0
A 2111	15h	39m	54.29s	34d	25m	06.60s		–18.05	–17.24	
A 2111	15h	39m	51.92s	34d	25m	18.80s		–18.85	–18.83	
A 2111	15h	39m	44.40s	34d	25m	22.70s		–19.46	–19.41	
A 2111	15h	39m	44.15s	34d	25m	21.30s		–18.78	–20.66	
A 2111	15h	39m	54.03s	34d	25m	24.60s		–18.87	–18.31	
A 2111	15h	39m	53.10s	34d	25m	26.50s		–18.75	–17.73	
A 2111	15h	39m	47.96s	34d	25m	32.10s		–20.49	–19.52	E
A 2111	15h	39m	52.98s	34d	25m	41.10s		–19.31	–18.24	
A 2111	15h	39m	43.94s	34d	25m	46.70s		–19.45	–19.01	
A 2111	15h	39m	42.69s	34d	25m	52.10s		–18.13	–16.99	
A 2111	15h	39m	42.04s	34d	26m	04.00s		–19.44	–18.39	

Table A.1. continued.

Name	α (J2000)			δ (J2000)			z	M_r	M_B	Morph
A 2111	15h	39m	42.02s	34d	25m	59.60s		–18.96	–20.78	
A 2111	15h	39m	44.85s	34d	25m	58.50s		–19.19	–19.08	
A 2111	15h	39m	47.82s	34d	26m	00.00s		–19.08	–18.05	
A 2111	15h	39m	53.40s	34d	25m	59.60s		–18.94	–18.56	
A 2111	15h	39m	52.50s	34d	26m	02.20s		–20.40	–19.62	S
A 2111	15h	39m	47.49s	34d	26m	11.10s		–18.84	–18.00	
A 2111	15h	39m	42.59s	34d	26m	14.00s		–19.82	–18.96	
A 2111	15h	39m	43.06s	34d	26m	23.00s		–18.42	–17.36	
A 2111	15h	39m	42.02s	34d	26m	30.30s	0.2258	–22.09	–20.96	E
A 2111	15h	39m	43.25s	34d	26m	32.90s		–19.02	–18.04	
A 2111	15h	39m	48.31s	34d	26m	36.70s		–18.79	–18.43	
A 2111	15h	39m	49.35s	34d	26m	41.50s	0.2299	–21.54	–21.03	S
A 2111	15h	39m	50.11s	34d	26m	44.40s		–19.48	–19.02	
A 2111	15h	39m	52.85s	34d	26m	46.80s		–20.45	–19.95	E
A 2111	15h	39m	42.09s	34d	26m	49.20s		–19.55	–18.52	
A 2111	15h	39m	45.75s	34d	26m	57.40s	0.2292	–21.07	–20.05	E
A 2111	15h	39m	42.98s	34d	27m	00.30s		–18.40	–18.28	
A 2111	15h	39m	42.30s	34d	27m	02.60s		–18.20	–17.92	
A 2111	15h	39m	52.55s	34d	27m	07.50s		–19.06	–20.58	
A 2111	15h	39m	52.04s	34d	27m	07.60s		–19.01	–21.29	
A 2111	15h	39m	52.15s	34d	27m	12.20s		–21.13	–21.23	S
A 2111	15h	39m	42.28s	34d	27m	17.10s		–20.12	–19.17	
A 2111	15h	39m	51.51s	34d	27m	31.30s		–19.54	–18.61	
A 2111	15h	39m	48.27s	34d	27m	34.80s		–18.70	–18.45	
A 2111	15h	39m	47.70s	34d	25m	16.40s		–19.85	–18.96	
A 2111	15h	39m	47.89s	34d	27m	39.90s		–20.28	–19.32	E
A 2111	15h	39m	47.34s	34d	25m	10.20s	0.2309	–21.07	–20.81	E
A 2111	15h	39m	47.26s	34d	25m	15.90s		–20.43	–20.38	S
A 1952	14h	41m	07.84s	28d	38m	29.40s		–22.05	–21.10	E
A 1952	14h	40m	59.08s	28d	38m	35.40s		–20.11	–19.24	S
A 1952	14h	41m	01.82s	28d	35m	57.10s		–20.13	–19.75	S
A 1952	14h	40m	59.60s	28d	36m	07.40s		–19.18	–18.44	
A 1952	14h	41m	02.64s	28d	36m	14.50s		–18.79	–18.40	
A 1952	14h	41m	01.57s	28d	36m	31.50s		–18.30	–18.20	
A 1952	14h	40m	59.42s	28d	36m	42.00s		–19.05	–18.36	
A 1952	14h	41m	04.07s	28d	36m	47.50s		–19.94	–19.04	E
A 1952	14h	41m	04.47s	28d	36m	49.70s		–18.71	–20.59	
A 1952	14h	41m	01.82s	28d	37m	09.60s		–18.17	–20.22	
A 1952	14h	41m	01.92s	28d	37m	14.50s		–20.76	–20.80	E
A 1952	14h	41m	02.66s	28d	37m	10.00s		–22.11	–21.94	S0
A 1952	14h	41m	03.13s	28d	37m	10.10s		–21.41	–20.84	E
A 1952	14h	41m	02.67s	28d	37m	02.40s		–20.63	–19.99	
A 1952	14h	40m	58.41s	28d	36m	52.50s		–19.89	–19.03	S0
A 1952	14h	41m	01.19s	28d	37m	00.50s		–21.20	–20.33	E
A 1952	14h	40m	59.94s	28d	37m	22.10s		–18.59	–17.95	
A 1952	14h	40m	59.55s	28d	37m	34.20s		–18.29	–17.81	
A 1952	14h	41m	01.81s	28d	37m	34.70s		–19.48	–18.91	
A 1952	14h	41m	01.58s	28d	37m	48.30s		–18.21	–20.37	
A 1952	14h	41m	01.32s	28d	37m	43.20s		–21.57	–21.82	E
A 1952	14h	41m	01.53s	28d	37m	44.30s		–19.21	–18.96	
A 1952	14h	40m	59.15s	28d	37m	47.80s		–18.93	–20.67	
A 1952	14h	40m	59.50s	28d	37m	48.80s		–19.90	–19.01	
A 1952	14h	40m	58.98s	28d	37m	51.40s		–18.41	–18.51	
A 1952	14h	41m	03.17s	28d	37m	52.50s		–18.10	–17.71	
A 1952	14h	40m	59.94s	28d	38m	00.10s		–20.38	–19.53	E
A 1952	14h	41m	08.82s	28d	37m	59.00s		–19.72	–19.04	E
A 1952	14h	41m	05.82s	28d	38m	02.20s		–18.68	–17.82	
A 1952	14h	41m	00.90s	28d	38m	04.70s		–19.54	–18.59	
A 1952	14h	41m	04.06s	28d	38m	08.40s		–19.13	–19.23	
A 1952	14h	41m	07.98s	28d	38m	09.40s		–19.08	–18.20	
A 1952	14h	41m	03.17s	28d	38m	21.10s		–18.04	–18.15	
A 1952	14h	41m	05.43s	28d	38m	21.80s		–19.11	–18.99	
A 1952	14h	41m	02.63s	28d	35m	50.80s		–18.52	–18.54	
A 1952	14h	40m	59.43s	28d	38m	27.20s		–19.17	–19.37	
A 1952	14h	41m	01.91s	28d	35m	54.80s		–19.06	–20.83	
A 1952	14h	40m	59.20s	28d	38m	24.20s		–19.32	–18.60	
A 1952	14h	41m	13.59s	28d	37m	29.60s		–22.13	–21.43	S0

Table A.1. continued.

Name	α (J2000)			δ (J2000)			z	M_r	M_B	Morph
A 1952	14h	41m	05.84s	28d	37m	41.60s		–20.22	–19.27	
A 1952	14h	41m	14.94s	28d	37m	42.60s		–21.80	–20.98	S0
A 1952	14h	41m	05.68s	28d	37m	46.70s		–18.22	–18.33	
A 1952	14h	41m	08.53s	28d	37m	49.00s		–19.26	–19.18	
A 1952	14h	41m	03.16s	28d	37m	52.20s		–18.08	–17.86	
A 1952	14h	41m	15.18s	28d	35m	29.10s		–18.16	–20.08	
A 1952	14h	41m	15.04s	28d	35m	21.20s		–19.32	–21.52	
A 1952	14h	41m	15.18s	28d	35m	24.30s		–19.61	–21.59	
A 1952	14h	41m	03.94s	28d	35m	21.30s		–20.35	–19.38	E
A 1952	14h	41m	13.55s	28d	35m	21.80s		–19.77	–19.72	
A 1952	14h	41m	05.92s	28d	35m	29.90s		–20.77	–19.82	S0
A 1952	14h	41m	08.36s	28d	35m	28.50s		–18.46	–18.64	
A 1952	14h	41m	08.59s	28d	35m	30.80s		–19.01	–19.42	
A 1952	14h	41m	08.51s	28d	35m	32.50s		–20.41	–20.52	S
A 1952	14h	41m	04.76s	28d	35m	32.40s		–19.40	–19.16	
A 1952	14h	41m	07.83s	28d	35m	32.30s		–18.39	–20.48	
A 1952	14h	41m	07.59s	28d	35m	35.00s		–21.58	–21.23	S
A 1952	14h	41m	11.01s	28d	35m	33.00s		–19.87	–18.93	
A 1952	14h	41m	10.10s	28d	35m	33.70s		–19.03	–18.15	
A 1952	14h	41m	05.91s	28d	35m	38.50s		–19.36	–18.50	
A 1952	14h	41m	08.19s	28d	35m	44.50s		–21.61	–20.93	S0
A 1952	14h	41m	03.56s	28d	35m	44.20s		–19.69	–19.45	
A 1952	14h	41m	13.72s	28d	35m	54.10s		–18.37	–18.45	
A 1952	14h	41m	13.55s	28d	35m	52.00s		–18.78	–21.38	
A 1952	14h	41m	03.27s	28d	35m	56.30s		–19.34	–18.51	
A 1952	14h	41m	08.00s	28d	36m	03.20s		–18.96	–18.97	
A 1952	14h	41m	09.73s	28d	36m	02.80s		–18.20	–17.44	
A 1952	14h	41m	05.67s	28d	36m	05.30s		–18.64	–17.72	
A 1952	14h	41m	12.15s	28d	36m	07.00s		–19.45	–18.73	
A 1952	14h	41m	10.72s	28d	36m	07.50s		–18.10	–18.28	
A 1952	14h	41m	14.47s	28d	36m	26.20s		–19.86	–19.18	
A 1952	14h	41m	05.45s	28d	36m	26.40s		–18.40	–17.58	
A 1952	14h	41m	04.06s	28d	36m	26.50s		–18.06	–20.09	
A 1952	14h	41m	04.22s	28d	36m	27.80s		–18.35	–19.37	
A 1952	14h	41m	12.94s	28d	36m	27.30s		–19.29	–18.61	
A 1952	14h	41m	06.81s	28d	36m	31.50s		–20.01	–21.90	E
A 1952	14h	41m	07.10s	28d	36m	37.30s		–20.67	–20.27	E
A 1952	14h	41m	07.03s	28d	36m	39.20s		–22.10	–22.55	S0
A 1952	14h	41m	03.36s	28d	36m	37.10s		–20.43	–19.40	E
A 1952	14h	41m	14.04s	28d	36m	40.80s		–18.80	–18.92	
A 1952	14h	41m	03.11s	28d	36m	46.60s		–20.74	–19.93	S0
A 1952	14h	41m	04.07s	28d	36m	52.70s		–19.32	–20.90	
A 1952	14h	41m	03.57s	28d	37m	00.30s		–22.61	–24.23	E
A 1952	14h	41m	03.14s	28d	36m	57.00s		–19.55	–21.16	
A 1952	14h	41m	10.75s	28d	36m	47.30s		–19.16	–21.67	
A 1952	14h	41m	06.34s	28d	37m	01.30s		–18.75	–18.04	
A 1952	14h	41m	06.48s	28d	37m	06.90s		–20.14	–19.23	
A 1952	14h	41m	08.25s	28d	37m	13.80s		–21.85	–21.21	S
A 1952	14h	41m	12.33s	28d	37m	11.00s		–19.03	–19.11	
A 1952	14h	41m	06.26s	28d	37m	12.20s		–18.15	–17.28	
A 1952	14h	41m	09.40s	28d	37m	13.00s		–18.55	–18.59	
A 1952	14h	41m	09.72s	28d	37m	17.80s		–19.85	–20.07	S
A 1952	14h	41m	05.02s	28d	37m	34.90s		–18.05	–20.08	
A 1952	14h	41m	06.27s	28d	37m	27.50s		–20.01	–20.84	S0
A 1952	14h	41m	05.49s	28d	37m	33.90s		–19.02	–21.47	
A 1952	14h	41m	05.32s	28d	37m	35.90s		–19.18	–20.34	
A 1952	14h	41m	04.78s	28d	37m	31.60s		–19.79	–21.64	
A 1952	14h	41m	04.76s	28d	37m	35.50s		–19.83	–19.94	
A 1952	14h	41m	04.77s	28d	35m	05.50s		–18.30	–18.55	
A 1952	14h	41m	06.32s	28d	37m	18.30s		–18.30	–17.78	
A 1952	14h	41m	14.57s	28d	37m	18.70s		–19.65	–19.37	
A 1952	14h	41m	11.82s	28d	37m	19.30s		–18.39	–18.59	
A 1952	14h	41m	07.53s	28d	37m	23.60s		–19.14	–18.20	
A 1952	14h	41m	04.29s	28d	37m	23.00s		–18.54	–18.27	
A 1952	14h	41m	05.23s	28d	35m	06.80s		–19.10	–18.75	
A 1952	14h	41m	03.35s	28d	37m	29.50s		–20.17	–19.26	
A 1952	14h	41m	06.39s	28d	37m	33.60s		–18.12	–17.60	

Table A.1. continued.

Name	α (J2000)			δ (J2000)			z	M_r	M_B	Morph
A 1952	14h	41m	12.23s	28d	35m	06.70s		–19.05	–18.27	
A 1952	14h	41m	08.44s	28d	35m	09.00s		–18.39	–17.78	
A 1952	14h	41m	05.36s	28d	37m	40.50s		–18.42	–17.71	
A 1952	14h	41m	10.78s	28d	35m	12.30s		–18.24	–18.05	
A 1952	14h	41m	13.01s	28d	35m	15.30s		–19.08	–19.23	
A 1952	14h	41m	10.45s	28d	35m	16.60s		–19.36	–19.26	
A 1952	14h	41m	14.88s	28d	35m	29.70s		–18.45	–19.98	